Results in Physics 10 (2018) 205–211

Contents lists available at ScienceDirect

Results in Physics

journal homepage: www.elsevier.com/locate/rinp

Study and investigation of phosphorus doping time on emitter region for contact resistance optimization of monocrystalline silicon solar cell

M.K. Basher[a,1], M. Khalid Hossain[a,*,1], R. Afaz[b], S. Tayyaba[c], M.A.R. Akand[a], M.T. Rahman[d], N.M. Eman[b]

[a] Institute of Electronics, Atomic Energy Research Establishment, Bangladesh Atomic Energy Commission, Dhaka 1349, Bangladesh
[b] Dept of Physics, University of Chittagong, Chittagong 4331, Bangladesh
[c] Dept of Computer Engineering, The University of Lahore, Lahore 54000, Pakistan
[d] Dept of Materials Science and Engineering, University of Rajshahi, Rajshahi 6205, Bangladesh

ARTICLE INFO

Keywords:
silicon solar cell
phosphorous diffusion
doping time
contact resistance
transmission line method
surface reflection measurement

ABSTRACT

In this paper, contact resistance of monocrystalline silicon solar cells was optimized by the variation of phosphorus doping time on emitter region. Wet-chemical texturization was performed to form pyramidal structure on silicon wafer surface. The surface morphology of the textured wafers was studied by field emission scanning electron microscope (FESEM) and surface reflection measurement (SRM). The textured wafers were doped by varying phosphorus doping time using constant flow rate of phosphorus oxychloride ($POCl_3$) in a high-temperature diffusion furnace. The phosphorus doped silicon wafers were metalized by screen printer using silver and aluminum paste in the front and back surface of the wafers respectively. To form ohmic contacts between silver/aluminum layer and the silicon wafer, rapid thermal annealing (RTA) was performed on the screen-printed solar cells. The contact resistance of screen-printed solar cells was measured using transmission line method (TLM). 25 minutes doped sample showed minimum front and back contact resistances, which could potentially be useful for efficient monocrystalline silicon solar cells fabrication.

Introduction

Harvesting of solar energy by solar cells has been increasing rapidly from last two decades as a substitute of fossil fuel-based energy sources [1–7]. The crystalline silicon solar cell is one of the dominant solar energy harvesting technology, where metallization of silicon wafer plays a crucial role in efficient collection of solar energy. For metallization, screen-printing is one the most suitable method in the photovoltaic industry because of its low fabrication cost, easy process, and quick metal deposition process with minimum environmental hazards [8,9]. Most of the larger scale solar cell production is based on metallization of doped emitter layer of silicon wafer [10]. The quality of the emitter, identified by measuring sheet resistance, plays a dominant role to enhance the photovoltaic performance [11,12]. Therefore, the emitter doping concentration (N_s) must be kept enough high (i.e., $N_s > 10^{19}$ atoms/cm^3) [13] to reduce the contact resistance (R_c) [14,15], which is the interface resistance between metallization materials and underneath semiconductor layer [9].

It is previously reported [10,16] that the quality of contacts between conductor and semiconductor materials plays a significant role for high-efficient solar cell. However, it is a challenging job to form an intimate contact between silver/aluminum and silicon without debasing the emitter region [10]. The formation of contact and its characteristics are influenced by the emitter doping level which may electrically active or inactive and a dead layer might be formed due to over doping [5]. Therefore, contact resistance becomes a matter of concern when emitter layer suffers from under or over doping. For this reason, optimization of doping time i.e. doping concentration is mandatory to get effective contact resistance [16]. But, the effect of contact resistance between conductor and semiconductor materials is rarely addressed in silicon solar cell research. Because of this, for the first time, we have investigated the effect of different phosphorus doping time on front and back contact resistances of the monocrystalline silicon solar cells.

In this research, monocrystalline silicon solar cells were fabricated by the variation of phosphorus doping time on emitter region, and then sheet resistance measurement was performed by four-point probe method to identify the changes of P-doping concentration with diffusion time. Also, contact resistance between the silver/aluminum layer

* Corresponding author.
E-mail address: khalid.baec@gmail.com (M. Khalid Hossain).
[1] Authors contributed equally to this work.

https://doi.org/10.1016/j.rinp.2018.05.038
Received 7 May 2018; Received in revised form 22 May 2018; Accepted 23 May 2018
Available online 01 June 2018

and silicon wafer was determined by using transmission line method (TLM) [17–19]. Finally, the optimized contact resistance is proposed for the fabrication of efficient silicon solar cells.

Materials and methods

In this work, six (6) p-type (1 0 0) oriented Czochralski monocrystalline silicon wafers were used. The thickness, area, and resistivity of the wafers were 200 μm, 127 × 127 mm^2, and 1–3 Ω.cm respectively. The wafers were cleaned and textured using the chemical solution of NaOH (1 g) + de-ionized H_2O (10 ml) and KOH (1 g) + IPA (5 ml) + de-ionized H_2O (125 ml) respectively for 10 min at 70 °C temperature. The purpose of cleaning and texturing the samples was to eliminate the surface contaminants and form the pyramidal structure on the wafer surface that could trap the incident light efficiently. Then the surface morphology and the optical surface reflection of the textured wafers were measured by FESEM (JSM-7600F) and SRM system. After that, phosphorous atoms were diffused into the p-type silicon wafers using phosphorous oxychloride by a high-temperature diffusion furnace (MRL PHOENIX, USA) to form the p-n junction. In this experiment, six (6) silicon wafer samples were doped with six different diffusion time such as 5, 10, 15, 20, 25, and 30 min respectively. The change of doping concentration with doping time was identified by measuring sheet resistance using four-point probe method. The sheet resistance of the wafer was measured from the five different positions of the doped wafer surface which have been already discussed elsewhere [11,12]. The P-type Si wafers before and after phosphorous diffusion are shown in Fig. 1 (a) and (b).

For contact resistance measurement, front and back side of the solar cells were metalized with silver and aluminum paste respectively using a TLM based printing screen [20,21]. The solar cell after screen printing is shown in Fig. 1(c). The screen-printed solar cells were placed in a preheated oven at 150 °C for 10 min so that the paste gets attached well to the wafer surface. Then the rapid thermal annealing (RTA) of screen-printed cells was performed at a maximum temperature of 820 °C which provided ohmic contact between the silver/aluminum and silicon wafers. Finally, the front and back contact resistances of the solar cells were determined using transmission line method (TLM).

Results and discussion

SEM analysis of textured wafer

To fabricate efficient silicon solar cell, surface texturization plays a vital role to reduce optical surface reflection by forming randomly distributed pyramid structure on the silicon wafer surface [22–24]. The textured wafer surface was analyzed by FESEM and the SEM images before and after texturization are shown in Fig. 2.

It is observed from Fig. 2(b) that, after texturing the wafer surface was fully covered with almost uniformly distributed pyramid structure. The formation of these pyramids was due to the anisotropy of the etch solution i.e. different crystal orientations are etched at different rates [25–28]. The pyramidal surface particularly plays a dominant role to reduce the optical surface reflection and favorable for efficient solar cell fabrication [23].

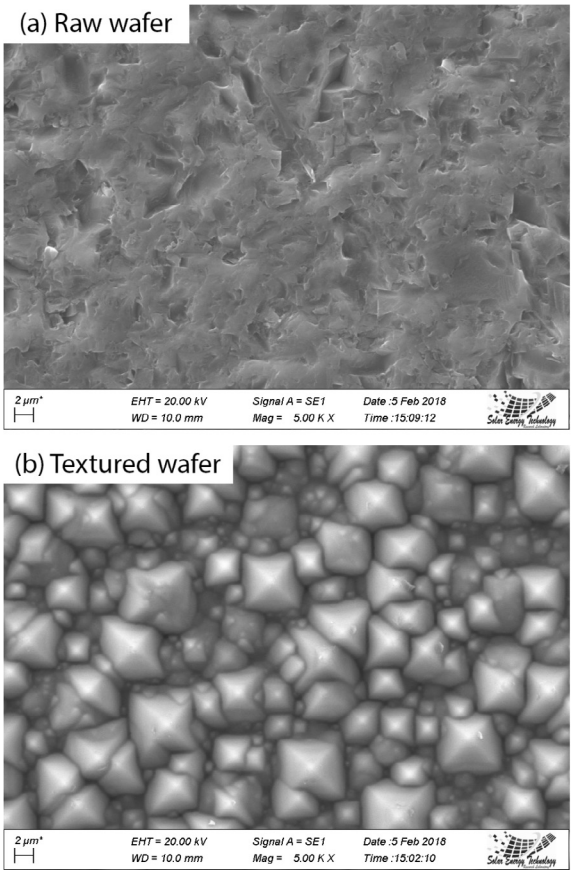

Fig. 2. SEM images for (a) raw wafer, and (b) textured wafer.

Analysis of surface reflection

Surface reflectance of the textured wafer was measured by collecting reflected light from the wafer surface as a function of wavelength using the surface reflectance measurement system. The graphical representation of optical reflectance data for the raw and textured wafers is shown in Fig. 3(a).

Fig. 3(a) shows that the percentage of reflectance decreases with increasing wavelength up to 500 nm and becomes almost constant between 500 and 1000 nm. Further increases of wavelength, the percentage of reflectance increases. It is observed that in the visible wavelength range (450–1000 nm), the reflectance decreases and the

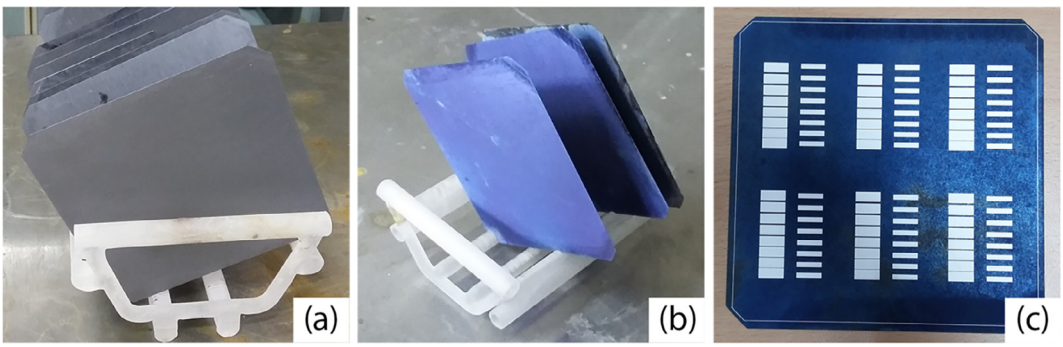

Fig. 1. (a) Raw (undoped) wafers, (b) phosphorous doped wafers, and (c) TLM based screen printed solar cell.

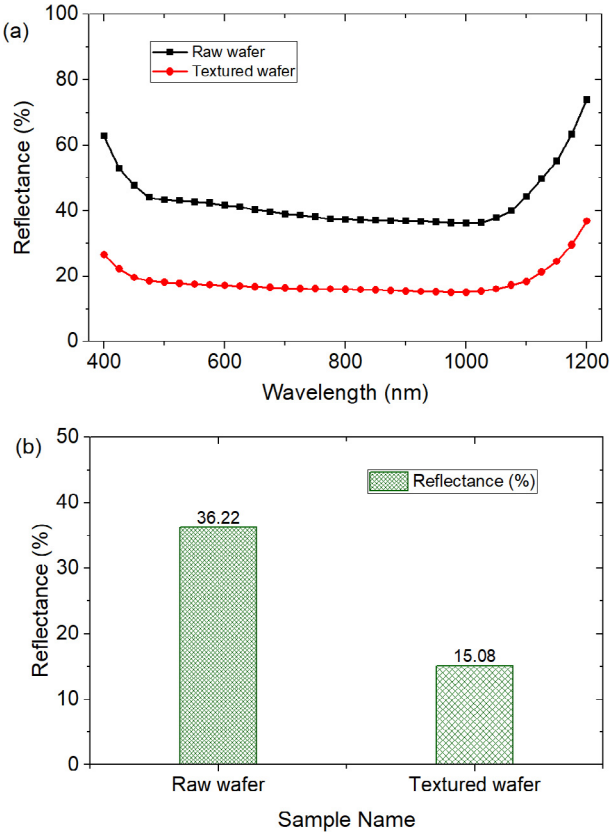

Fig. 3. (a) Reflectance versus wavelength curve of wafer, (b) percentage of reflectance values of raw wafer and textured wafer.

minimum reflectance becomes 15.08%. The percentage values of reflectance of both raw wafer and textured wafer are shown in Fig. 3(b). It is observed that surface reflection reduced from 36.22% to 15.08% due to anisotropic etching of monocrystalline silicon wafers [25,26]. The lower optical reflectance mostly depends on the shape, size, and uniformity of the pyramids on the wafer surface [29]. The pyramidal structures are governed by the optimum etching time, potassium hydroxide (KOH), and isopropyl alcohol (IPA) where etching time nucleate the pyramids, KOH helps to increase the number of pyramids and IPA is responsible for growing big pyramids [25,30].

Analysis of sheet resistance

Sheet resistance exhibits crucial role in silicon solar cell fabrication because it indicates the quality and uniformity of emitter doping region [11]. By measuring the sheet resistance, it is easy to identify the quality of the doped wafer because heavily doped wafer gives lower sheet resistance whether lightly doped wafer gives higher sheet resistance. Furthermore, the uniformity of the doped wafer can also be identified by measuring sheet resistance from the different positions [11]. In this study, the sheet resistances of pre-doped (raw wafer) and post-doped Si wafers was measured and presented in Table 1 and Fig. 4.

Generally, undoped or weakly shallow junction causes the high sheet resistance resulting high contact resistance in the silicon wafer. On the other hand, heavily doped emitter leads to low sheet resistance resulting in the reduced contact resistance [14,15]. From Fig. 4 it is observed that the sheet resistance of all the wafers was decreased significantly while doped with phosphorus atoms. The sheet resistance before diffusion of the wafer was found 7578 Ω/□ which sharply decreased to 143, 119, 92, 65, 42, and 150 Ω/□ for the post-diffused wafer 1, wafer 2, wafer 3, wafer 4, wafer 5, and wafer 6 respectively. These lower sheet resistances are favorable for improving the efficiency

Table 1
Sheet resistances of the wafers for different diffusion time.

Wafer name	Diffusion time (min)	Sheet resistance (Ω/□)
Raw wafer	0	7578
Wafer 1	5	142
Wafer 2	10	119
Wafer 3	15	92
Wafer 4	20	65
Wafer 5	25	42
Wafer 6	30	150

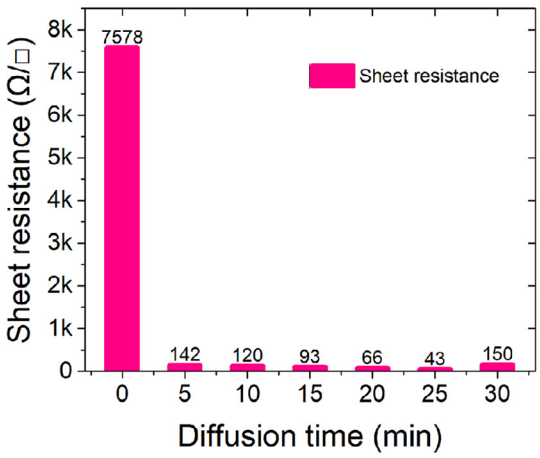

Fig. 4. Variation of sheet resistance with diffusion time.

of a solar cell. It is also seen that sheet resistance decreases during increasing of diffusion time until 25 min. Since higher diffusion time helps to increase doping concentration of phosphorus atoms, sheet resistance has a reciprocal relationship with doping concentration [31]. However, at 30 min of diffusion time, sheet resistance started to increase again which may be due to over doping. An extreme high densitie of phosphorus atom from a doping source sometimes formed a doped emitter region, where solid solubility limits may be exceeded [31–33]. From the previous study, it is found that the excess phosphorus atoms create a defect source that makes the emitter electrically inactive or dead [10,34–36]. This dead layer is the major recombination source of photogenerated carriers in the crystalline silicon solar cells due to the increment of defect densities [37,38], resulting in the lower conversion efficiency [33,39].

Analysis of font contact resistance

The front contact resistances of the fabricated six monocrystalline silicon solar cells were measured by transmission line method (TLM). From six pattern areas [20,21] (Area 1 to Area 6) of each sample, the linear regression analysis curve drawn from TLM resistance data for the front side of sample 1, 2, 3, 4, 5 and 6 which are shown in Fig. 5(a)–(f). Using linear regression analysis, the intercept of Fig. 5(a) for area 1 of sample 1 was calculated. By using the contact resistance formula, it is found that the front contact resistance for the TLM pattern area 1 of sample 1 is 28.328 Ω. In a similar way, contact resistances for the TLM pattern area 2, 3, 4, 5, and 6 become 27.653 Ω, 28.260 Ω, 27.475 Ω, 27.515 Ω, and 27.506 Ω respectively. The average front contact resistance of sample 1 is 27.789 Ω. Following the similar way, the front contact resistances of sample 2, sample 3, sample 4, sample 5, and sample 6 were calculated. The summary of the front contact resistances for TLM patterns [20,21] of six samples is shown in Table 2.

In this research, six samples were doped with phosphorous atoms with the time variation of 5 min, 10 min, 15 min, 20 min, 25 min, and 30 min and the corresponding front contact resistances were found

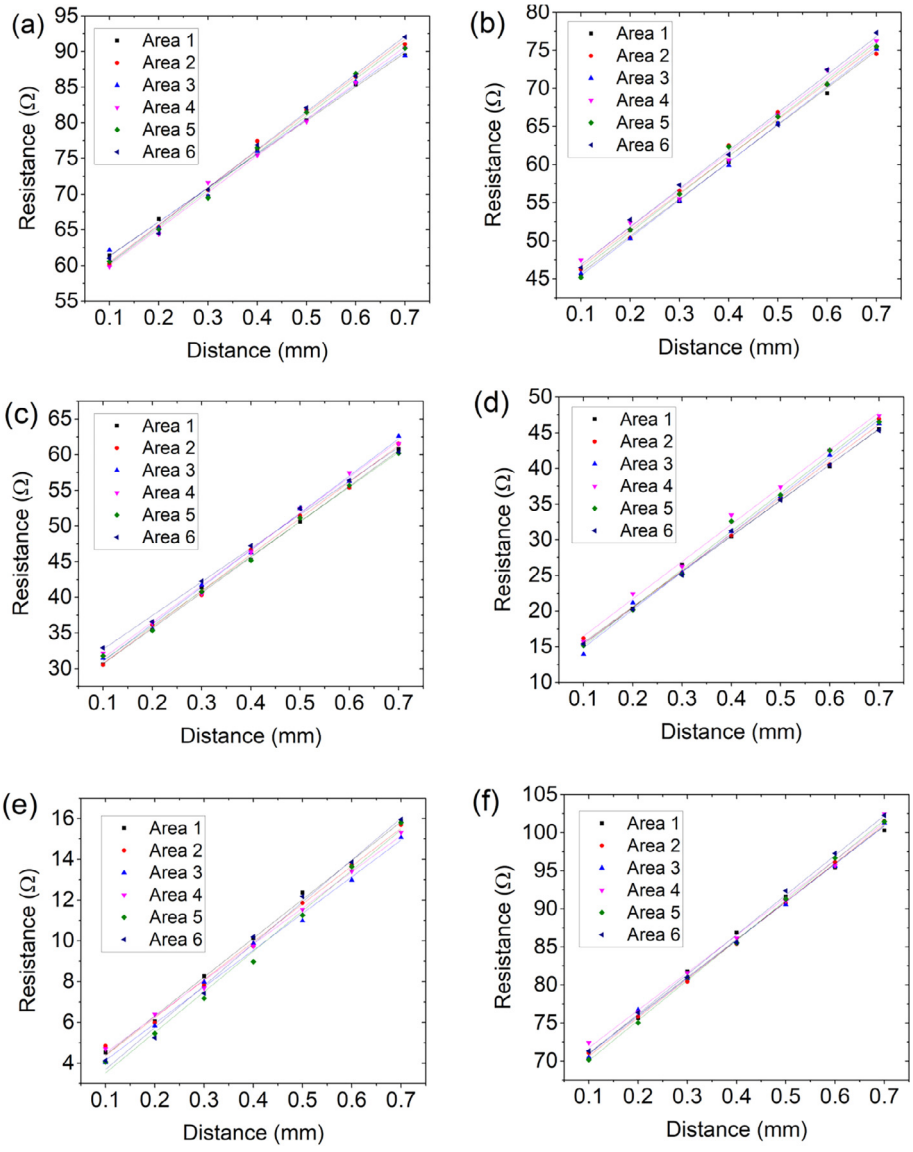

Fig. 5. Linear regression analysis curve drawn from TLM resistance data for the front side of sample 1, 2, 3, 4, 5 and 6.

Table 2
Summary of the front contact resistances of TLM pattern for six samples.

Sample name	Contact resistance of front side [Ω]						
	Area 1	Area 2	Area 3	Area 4	Area 5	Area 6	Average
Sample 1	28.32	27.65	28.26	27.47	27.51	27.50	27.78
Sample 2	20.44	20.87	20.23	20.97	20.57	20.92	20.67
Sample 3	12.84	12.82	12.92	13.20	13.13	14.01	13.15
Sample 4	5.319	5.151	4.77	5.63	4.88	5.19	5.15
Sample 5	1.252	1.256	1.16	1.36	0.76	0.82	1.10
Sample 6	33.03	32.78	32.95	33.41	32.40	32.87	32.91

27.789 Ω, 20.672 Ω, 13.157 Ω, 5.159 Ω, 1.105 Ω, and 32.911 Ω respectively. The change in front contact resistance with diffusion time is shown in Fig. 6. From the Fig. 6, it is seen that the front contact resistance decreases with phosphorous doping time i.e. doping concentration increases. It is also observed that the front contact resistance started to decrease when doping time was 5 min and continued until 25 min where the contact resistance was minimum. Beyond this doping time, a dead layer was formed on silicon wafer surface [35,36]. From the Table 2 and Fig. 6 it is clear that the minimum contact resistance

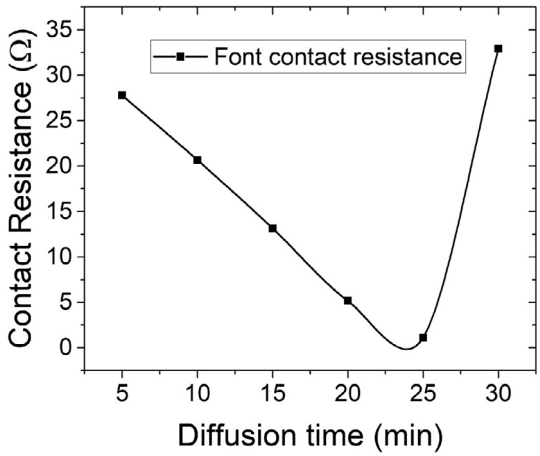

Fig. 6. Contact resistance versus diffusion time curve for the front side of solar cells.

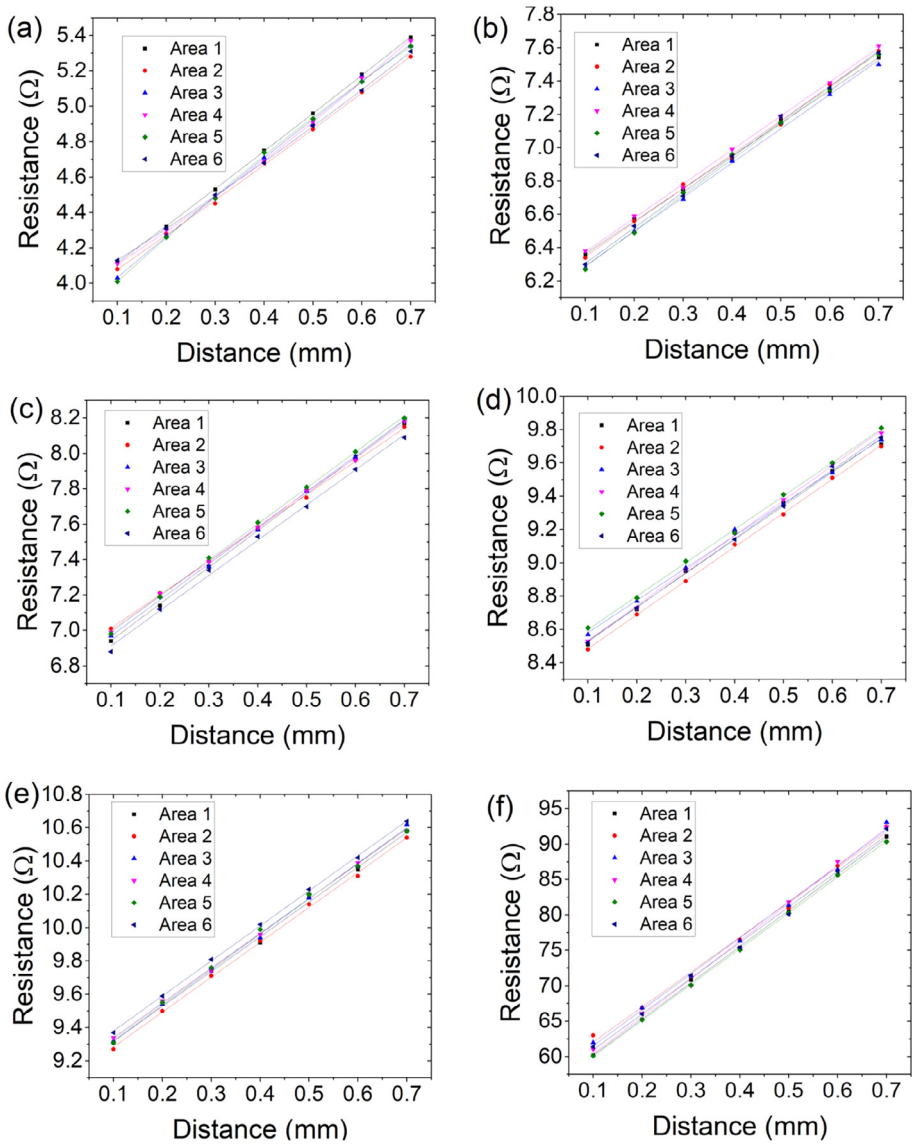

Fig. 7. Linear regression analysis curve is drawn from TLM resistance data for the back side of sample 1, 2, 3, 4, 5 and 6.

was found at 25 min doping time and above this doping time such as 30 min, a dead layer was formed which is considered as an electrically isolated region [10,34]. Therefore, for the optimum diffusion time of 25 min, the minimum front contact resistance becomes 1.105 Ω, which is compatible with efficient silicon solar cells.

Analysis of back contact resistance

The back contact resistances of the fabricated six monocrystalline silicon solar cells were measured by TLM. From six pattern areas (Area 1 to Area 6) of each sample, the linear regression analysis curve drawn from TLM resistance data for the back side of sample 1, 2, 3, 4, 5 and 6 are shown in Fig. 7(a)–(f). The back contact resistance was calculated by the similar way as the front contact resistance was measured. The summary of the back contact resistance of TLM patterns for six samples is shown in Table 3. The average back contact resistance for the six samples was found 1.933 Ω, 3.061 Ω, 3.386 Ω, 4.170 Ω, 4.560 Ω, and 27.886 Ω for their corresponding time variation. Also, the change in back contact resistance with diffusion time is shown in Table 3 and Fig. 8.

From Fig. 8 it is observed that back contact resistance increases slowly with increasing doping time up to 25 min and after that, it increases very sharply. This rapid increase of resistance may be due to exceeding the solid solubility limit of phosphorous atoms in silicon wafers. As a result, 30 min doping time shows the maximum contact resistance, which produces a dead layer or electrically isolated layer [35,36]. Therefore, 25 min diffusion time could be considered as optimized time, which would be favorable for the fabrication of efficient monocrystalline silicon solar cell.

Table 3
Summary of the back contact resistances of TLM pattern for six samples.

Sample name	Contact resistance of front side [Ω]						
	Area 1	Area 2	Area 3	Area 4	Area 5	Area 6	Average
Sample 1	1.94	1.93	1.91	1.93	1.90	1.95	1.93
Sample 2	3.08	3.07	3.04	3.08	3.03	3.04	3.06
Sample 3	3.36	3.41	3.38	3.40	3.39	3.35	3.38
Sample 4	4.16	4.14	4.19	4.16	4.19	4.16	4.17
Sample 5	4.55	4.53	4.55	4.56	4.56	4.58	4.56
Sample 6	27.54	28.56	28.22	27.52	27.49	27.96	27.88

The contact resistance is affected by three main factors: (a) semiconductor materials, (b) doping concentration, and (c) type of conductor materials [40]. There are also some other factors which may

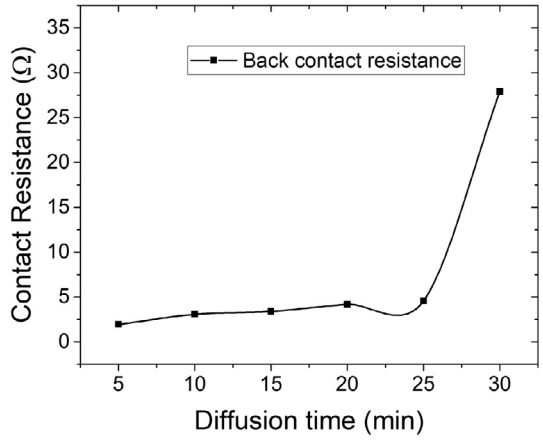

Fig. 8. Contact resistance versus diffusion time curve for the backside of solar cells.

affect the contact resistance, such as metallization materials quality, firing recipe and air quality of the laboratory [10,11]. However, the doping concentration is the significant factor which controls the contact resistance [31,41]. Higher doping density reduces the contact resistance significantly, but over doping produces “dead layer” on the semiconductor surface. This dead layer is formed when concentration of phosphorous atoms exceeds the solid solubility limit of silicon and makes the silicon electrically inactive [31,33]. The dead layer also acts as a recombination center which is generally responsible for increasing the Shockley-Read-Hall recombination and thus the performance of solar cell could be hampered [38,39,42,43].

It is seen that front contact resistance decreases with the increase of doping time, whereas, back contact resistance increases with the increases of doping time. The possible reason is that after diffusion the structure of the wafer becomes n^+-p-n^+, but for making a solar cell, the back side n^+ layer must be made the p^+ layer. But for making an efficient solar cell, the back side layer must be made by p^+ layer rather n^+ layer. The aluminum paste was used to make the p^+ layer on the back side of the silicon wafer by over doping the n+ layer. As phosphorus doping concentration increased with time but aluminum concentration remains fixed, thus back contact resistance increased with doping time.

Conclusions

In this research, silicon solar cells were fabricated on p-type monocrystalline silicon wafers by varying phosphorus doping time on emitter region. The wet-chemical texturization of (1 0 0) oriented silicon wafer produced (1 1 1) oriented pyramidal surface, which reduces the optical reflectance from 36.22% to 15.08%. This reduction in surface reflectance could be utilized to improve the absorbance and photoconversion efficiency of monocrystalline silicon solar cells. The sheet resistance measurement identified the proper and uniform doping concentration of phosphorus atoms on the silicon wafers. The decrement of sheet resistance confirmed the increment of phosphorus doping concentration with diffusion time. The contact resistance ensured its dependency on phosphorus doping time. This study unveiled that the contact resistance increases at the front side and decreases at the back side of the wafers at higher doping concentration until the dead layer of phosphorus atoms formed. The optimized front and back contact resistances were found 1.105 Ω and 4.560 Ω respectively at 25 min of doping time without dead layer creation, may compatible with efficient monocrystalline silicon solar cells.

Author contributions

M. K. Basher and M. Khalid Hossain designed the concept, and R. Afaz conducted the experiments. M. K. Basher and M. Khalid Hossain wrote the main manuscript text and all authors reviewed the paper.

Conflicts of interest

The authors declare that they have no competing interests.

Acknowledgement

The authors are grateful to IFRD, BCSIR for SEM analysis, and thankful to Institute of Electronics of Bangladesh Atomic Energy Commission to support this work.

References

[1] Hossain MK, Mortuza AA, Sen SK, Basher MK, Ashraf MW, Tayyaba S, et al. A comparative study on the influence of pure anatase and Degussa-P25 TiO_2 nanomaterials on the structural and optical properties of dye sensitized solar cell (DSSC) photoanode. Optik (Stuttg) 2018. http://dx.doi.org/10.1016/j.ijleo.2018.05.032.
[2] Hossain MK, Pervez MF, Mia MNH, Mortuza AA, Rahaman MS, Karim MR, et al. Effect of dye extracting solvents and sensitization time on photovoltaic performance of natural dye sensitized solar cells. Results Phys 2017;7:1516–23. http://dx.doi.org/10.1016/j.rinp.2017.04.011.
[3] Qarony W, Hossain MI, Hossain MK, Uddin MJ, Haque A, Saad AR, et al. Efficient amorphous silicon solar cells: characterization, optimization, and optical loss analysis. Results Phys 2017;7:4287–93. http://dx.doi.org/10.1016/j.rinp.2017.09.030.
[4] Hossain MK, Pervez MF, Tayyaba S, Uddin MJ, Mortuza AA, Mia MNH, et al. Efficiency enhancement of natural dye sensitized solar cell by optimizing electrode fabrication parameters. Mater Sci 2017;35:816–23. http://dx.doi.org/10.1515/msp-2017-0086.
[5] Hossain MI, Qarony W, Hossain MK, Debnath MK, Uddin MJ, Tsang YH. Effect of back reflectors on photon absorption in thin-film amorphous silicon solar cells. Appl Nanosci 2017;7:489–97. http://dx.doi.org/10.1007/s13204-017-0582-y.
[6] Hossain MK, Pervez MF, Uddin MJ, Tayyaba S, Mia MNH, Jewel MKH, et al. Influence of natural dye adsorption into TiO_2 based DSSC's photoanode on structural, morphological and optical properties. Mater Sci 2018;36:93–101. http://dx.doi.org/10.1515/msp-2017-0090.
[7] Hossain MK, Pervez MF, Mia MNH, Tayyaba S, Uddin MJ, Ahamed R, et al. Annealing temperature effect on structural, morphological and optical parameters of mesoporous TiO_2 film photoanode for dye-sensitized solar cell application. Mater Sci 2017;35:868–77. http://dx.doi.org/10.1515/msp-2017-0082.
[8] Recart F, Freire I, Pérez L, Lago-Aurrekoetxea R, Jimeno JC, Bueno G. Screen printed boron emitters for solar cells. Sol Energy Mater Sol Cells 2007;91:897–902. http://dx.doi.org/10.1016/j.solmat.2007.02.005.
[9] Vinod PN. Specific contact resistance measurement of screen-printed Ag metal contacts formed on heavily doped emitter region in multicrystalline silicon solar cells. J Electron Mater 2013;42:2905–9. http://dx.doi.org/10.1007/s11664-013-2678-9.
[10] Cabrera E, Olibet S, Rudolph D, Vullum PE, Kopecek R, Reinke D, et al. Impact of excess phosphorus doping and Si crystalline defects on Ag crystallite nucleation and growth in silver screen-printed Si solar cells. Prog Photovoltaics Res Appl 2015;23:367–75. http://dx.doi.org/10.1002/pip.2440.
[11] Jia H, Luo L, Jiang Y, Xu Z, Ren X, Zhang C. Diffusion process for efficiency improvement with high sheet resistance on traditional production lines of solar cell. Sci China Technol Sci 2014;57:962–7. http://dx.doi.org/10.1007/s11431-014-5520-6.
[12] Yang Y, Seyedmohammadi S, Kumar U, Gnizak D, Graddy ED, Shaikh A. Screen printable silver paste for silicon solar cells with high sheet resistance emitters. Energy Proc 2011;8:607–13. http://dx.doi.org/10.1016/j.egypro.2011.06.190.
[13] Schroder DK, Meie DL. Solar cell contact resistance—A review. IEEE Trans Electron Devices 1984;31:637–47.
[14] Glunz SW. High-efficiency crystalline silicon solar cells. Adv Optoelectron 2007;2007:1–15. http://dx.doi.org/10.1155/2007/97370.
[15] Nijs J, Sivoththaman S, Szlufcik J, De Clercq K, Duerinckx F, Van Kerschaever E, et al. Overview of solar cell technologies and results on high efficiency multicrystalline silicon substrates. Sol Energy Mater Sol Cells 1997;48:199–217. http://dx.doi.org/10.1016/S0927-0248(97)00103-7.
[16] Vinod PN, Chakravarty BC, Lal M, Kumar R, Singh SN. A novel method for the determination of the front contact resistance in large area screen printed silicon solar cells. Semicond Sci Technol 2000;15:286–90. http://dx.doi.org/10.1088/0268-1242/15/3/311.
[17] Proctor SJ, Linholm LW. A direct measurement of interfacial contact resistance. IEEE Electron Device Lett 1982;3:294–6.
[18] Guo S, Gregory G, Gabor AM, Schoenfeld WV, Davis KO. Detailed investigation of TLM contact resistance measurements on crystalline silicon solar cells. Sol Energy 2017;151:163–72. http://dx.doi.org/10.1016/j.solener.2017.05.015.
[19] Janoch R, Gabor AM, Anselmo A, Dube CE. Contact resistance measurement –

observations on technique and test parameters. 2015 IEEE 42nd Photovolt. Spec. Conf., IEEE; 2015, p. 1–6. doi:10.1109/PVSC.2015.7355851.
[20] Sahoo KC, Chang C-W, Wong Y-Y, Hsieh T-L, Chang EY, Lee C-T. Novel Cu/Cr/Ge/Pd ohmic contacts on highly doped n-GaAs. J Electron Mater 2008;37:901–4. http://dx.doi.org/10.1007/s11664-008-0398-3.
[21] Shih Y-C, Shao Y, Shi FG. Novel ceramic additives for screen-printable silicon solar cell metallization. J Electron Mater 2016;45:3999–4004. http://dx.doi.org/10.1007/s11664-016-4631-1.
[22] Iyengar VV, Nayak BK, Gupta MC. Optical properties of silicon light trapping structures for photovoltaics. Sol Energy Mater Sol Cells 2010;94:2251–7. http://dx.doi.org/10.1016/j.solmat.2010.07.020.
[23] Kwon S, Yi J, Yoon S, Lee JS, Kim D. Effects of textured morphology on the short circuit current of single crystalline silicon solar cells: Evaluation of alkaline wet-texture processes. Curr Appl Phys 2009;9:1310–4. http://dx.doi.org/10.1016/j.cap.2008.12.014.
[24] Chu AK, Wang JS, Tsai ZY, Lee CK. A simple and cost-effective approach for fabricating pyramids on crystalline silicon wafers. Sol Energy Mater Sol Cells 2009;93:1276–80. http://dx.doi.org/10.1016/j.solmat.2009.01.018.
[25] Xi Z, Yang D, Dan W, Jun C, Li X, Que D. Investigation of texturization for monocrystalline silicon solar cells with different kinds of alkaline. Renew Energy 2004;29:2101–7. http://dx.doi.org/10.1016/j.renene.2004.03.003.
[26] Ma X, Liu Z, Liao H, Li J. Surface texturisation of monocrystalline silicon solar cells. 2011 Asia-Pacific Power Energy Eng. Conf., IEEE; 2011, p. 1–4. doi:10.1109/APPEEC.2011.5748892.
[27] Abdur-Rahman E, Alghoraibi I, Alkurdi H. Effect of isopropyl alcohol concentration and etching time on wet chemical anisotropic etching of low-resistivity crystalline silicon wafer. Int J Anal Chem 2017;2017:1–9. http://dx.doi.org/10.1155/2017/7542870.
[28] Velidandla V, Xu J, Hou Z, Wijekoon K, Tanner D. Texture process monitoring in solar cell manufacturing using optical metrology. 2011 37th IEEE Photovolt. Spec. Conf., IEEE; 2011, p. 001744–7. doi:10.1109/PVSC.2011.6186291.
[29] Han K-M, Yoo J-S. Wet-texturing process for a thin crystalline silicon solar cell at low cost with high efficiency. J Korean Phys Soc 2014;64:1132–7. http://dx.doi.org/10.3938/jkps.64.1132.
[30] Papet P, Nichiporuk O, Kaminski A, Rozier Y, Kraiem J, Lelievre J-F, et al. Pyramidal texturing of silicon solar cell with TMAH chemical anisotropic etching. Sol Energy Mater Sol Cells 2006;90:2319–28. http://dx.doi.org/10.1016/j.solmat.2006.03.005.
[31] Shen L, Liang ZC, Liu CF, Long TJ, Wang DL. Optimization of oxidation processes to improve crystalline silicon solar cell emitters. AIP Adv 2014;4:27127. http://dx.doi.org/10.1063/1.4866981.
[32] Lee HJ, Kang MG, Choi SJ, Kang GH, Myoung JM, Song H. Characteristics of silicon solar cell emitter with a reduced diffused phosphorus inactive layer. Curr Appl Phys 2013;13:1718–22. http://dx.doi.org/10.1016/j.cap.2013.06.020.
[33] Kumar D, Saravanan S, Suratkar P. Effect of oxygen ambient during phosphorous diffusion on silicon solar cell. J Renew Sustain Energy 2012;4:33105. http://dx.doi.org/10.1063/1.4717513.
[34] Armigliato A, Nobili D, Servidori M, Solmi S. SiP precipitation within the doped silicon lattice, concomitant with phosphorus predeposition. J Appl Phys 1976;47:5489–91. http://dx.doi.org/10.1063/1.322549.
[35] Solmi S, Nobili D. High concentration diffusivity and clustering of arsenic and phosphorus in silicon. J Appl Phys 1998;83:2484–90. http://dx.doi.org/10.1063/1.367008.
[36] Nobili D, Armigliato A, Finnetti M, Solmi S. Precipitation as the phenomenon responsible for the electrically inactive phosphorus in silicon. J Appl Phys 1982;53:1484–91. http://dx.doi.org/10.1063/1.330646.
[37] Richter A, Werner F, Cuevas A, Schmidt J, Glunz SW. Improved parameterization of auger recombination in silicon. Energy Proc 2012;27:88–94. http://dx.doi.org/10.1016/j.egypro.2012.07.034.
[38] Ostoja P, Guerri S, Negrini P, Solmi S. The effects of phosphorus precipitation on the open-circuit voltage in N+/P silicon solar cells. Sol Cells 1984;11:1–12. http://dx.doi.org/10.1016/0379-6787(84)90114-5.
[39] Wagner H, Dastgheib-Shirazi A, Min B, Morishige AE, Steyer M, Hahn G, et al. Optimizing phosphorus diffusion for photovoltaic applications: Peak doping, inactive phosphorus, gettering, and contact formation. J Appl Phys 2016;119:185704. http://dx.doi.org/10.1063/1.4949326.
[40] Jäger U, Thaidigsmann B, Okanovic M, Preu R. Quantum efficiency analysis of highly doped areas for selective emitter solar cells. Energy Proc 2011;8:193–9. http://dx.doi.org/10.1016/j.egypro.2011.06.123.
[41] Chen N, Tate K, Ebong A. Generalized analysis of the impact of emitter sheet resistance on silicon solar cell performance. Jpn J Appl Phys 2015;54. http://dx.doi.org/10.7567/JJAP.54.08KD20.
[42] Min B, Wagner H, Dastgheib-Shirazi A, Altermatt PP. Limitation of industrial phosphorus-diffused emitters by SRH recombination. Energy Proc 2014;55:115–20. http://dx.doi.org/10.1016/j.egypro.2014.08.090.
[43] Min B, Wagner H, Dastgheib-Shirazi A, Kimmerle A, Kurz H, Altermatt PP. Heavily doped Si:P emitters of crystalline Si solar cells: recombination due to phosphorus precipitation. Phys Status Solidi Rapid Res Lett 2014;8:680–4. http://dx.doi.org/10.1002/pssr.201409138.